PSSP WAVES - THEIR PRESENCE AND POSSIBLE UTILIZATION IN SEISMIC INVERSION

LARRY LINES[1], PATRICK DALEY[1], JOAN EMBLETON[1] and DAVID GRAY[2]

[1] *CHORUS, Department of Geoscience, University of Calgary, Calgary, Alberta, Canada T2N 1N4. lrlines@ucalgary.ca*
[2] *Nexen Energy ULC, a CNOOC Limited Company, Calgary, Alberta, Canada T2P 3P7.*

(Received June 20, 2016; accepted September 29, 2016)

ABSTRACT

Lines, L.R., Daley, P.F., Embleton, J. and Gray, D., 2016. PSSP waves - their presence and possible utilization in seismic inversion. *Journal of Seismic Exploration*, 25: 497-512.

While the interpretation of reflected P-waves on seismic data remains the main vehicle for seismic interpretation, there are other signals in seismic reflection recordings that are not fully utilized in seismic inversion. There are reflection signals that are due to the conversion of P-wave energy to S-wave energy in transmission followed by conversion from S-wave to P-wave upon reflection. These waves, known as PSSP waves, have significant amplitude and normal moveout and are seen on reflection records at wide offset. We model PSSP waves by ray tracing and finite-difference wave equation computations. While PSSP amplitudes are essentially zero at normal incidence for flat reflectors, their energy is considerable at larger offsets. In addition to the identification of the PSSP modes, there is the challenge of utilizing this energy for estimation of seismic velocities. While the NMO for PSSP arrivals allows it to be suppressed through stacking in imaging P-wave reflections, it is feasible that full waveform inversion could utilize the PSSP energy as useful signal rather than treating it as undesirable "noise".

KEY WORDS: PSSP converted waves, full waveform inversion.

INTRODUCTION

The presence of PSSP waves on seismic data

Conventional seismic processing and interpretation has traditionally involved the analysis of P-waves that have undergone a single reflection. Converted mode seismic arrivals will generally not be handled appropriately with conventional seismic processing methods.

0963-0651/16/$5.00

However, seismic recordings may often contain converted mode signals as shown by the examples from Jones (2014). Jones showed that reflections from chalk formations contain not only P-wave reflections but contain useful converted wave arrivals (PPSP + PSPP, and PSSP) arrivals as well.

Recently, Nexen Inc. has provided a seismic data example (Fig. 1) from the Long Lake area of the Athabasca oil sands region that shows reflection events with almost zero amplitude at normal incidence and with considerably more normal moveout (NMO) than neighbouring P-wave reflections. The NMO and increasing amplitude variation with offset suggest that these are waves that involve conversion from P to S energy. The converted wave arrivals are confirmed by both ray tracing and elastic wave finite-difference modeling.

Elastic wave models of dipole sonic logs for this area are shown in Fig.2. The figure shows a series of shot gathers for shots spaced 10 m apart with receiver offsets from 0 to 1000 m. There are arrivals in the reservoir zone at about 465 ms, indicated by the arrow in Fig. 1, that have considerable more NMO than reflection arrivals above and below the reservoir zone. The NMO is considered to be too large for that of an interbed P-wave multiple, since the

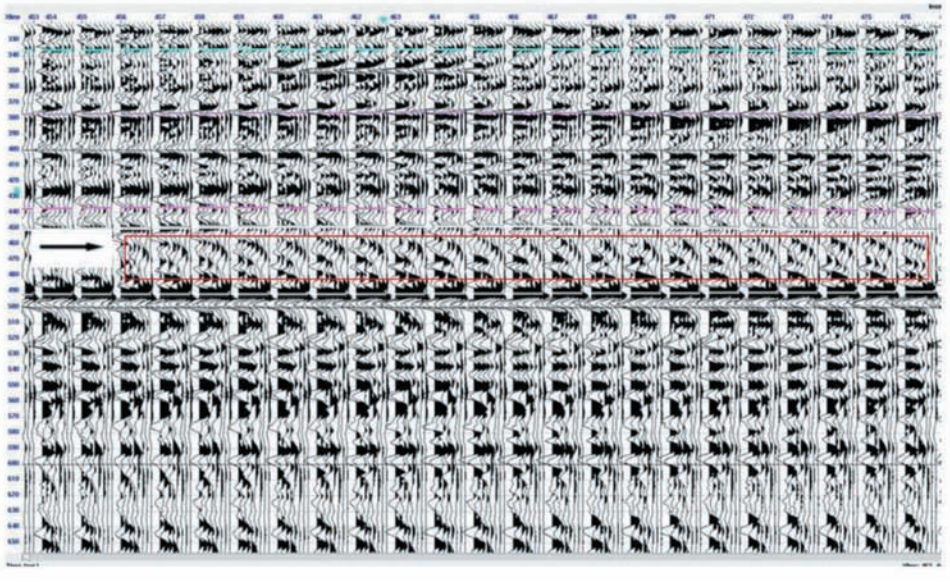

Fig. 1. Seismic shot gathers from the Nexen Long Lake field for shots separated by 10 m and receiver offsets from 0 - 1000 m. The arrow at 465 ms points to a series of reflection events that have large NMO and amplitudes that increase with offset. It is believed that these are PSSP arrivals.

P-wave velocities both above and below the reservoir zone would create multiples with much less NMO. We also note that these arrivals in the shot gathers have weak amplitudes at near offset and the amplitudes increase with increasing offset. Given the NMO and amplitude variation, it is believed that these arrivals are PSSP arrivals and this will be verified by seismic modeling. It is believed that these PSSP arrivals could provide useful information about the subsurface.

In this study we develop a layered model based on blocking dipole sonic logs from the Long Lake area (Lines et al., 2010), and use this model in the computation of elastic wave synthetic seismograms. The synthetic seismograms utilize elastic wave finite-difference codes as described by Levander (1988) and asymptotic ray theory codes as developed by Daley and Krebes (2015).

These seismic modeling codes are used jointly to identify converted seismic modes such as PSSP. We confirm and predict the location of converted modes on reflection seismograms. Traditionally, the converted wave energy has often been suppressed in conventionally processing through NMO-stacking to enhance the P-wave reflection energy. We discuss how we might utilize the PSSP energy and other converted modes through the process of full waveform inversion.

A VELOCITY MODEL

The model for P-wave and S-wave velocities in this study is based on the blocking of sonic logs from the Long Lake area, as shown in Lines et al. (2010). The model basically has 3 layers based on the blocking of sonic logs and is shown schematically in Fig. 2. This velocity model is summarized in Table 1.

Table 1. Three-layer model for seismic modeling based on Long Lake dipole sonics.

Formation	Formation Top Depth	P-wave velocity	S-wave velocity	Density
Post-McMurray	0 m	2000 m/s	800 m/s	2.073 g/cm^3
McMurray	120 m	2400 m/s	960 m/s	2.170 g/cc^3
Devonian	190 m	3500 m/s	1750 m/s	2.384 g/cm^3

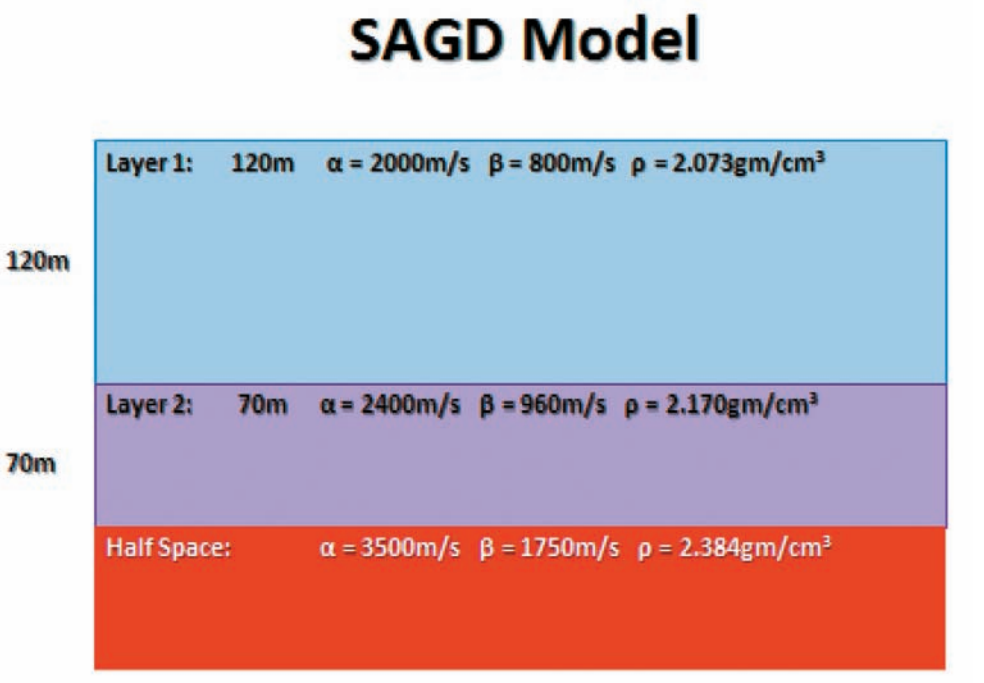

Fig. 2. Velocity-depth model based on blocking of dipole sonic logs from Lines et al. (2010).

Ray traced modes of P- and S-wave conversions

To appreciate the nature of purely P-wave reflections (such as PPPP) and converted wave arrivals (such as PSSP), we model these waves by using asymptotic ray tracing and finite-difference wave equation modeling. It is instructive to perform both types of modeling since ray tracing allows us to isolate reflection events whereas finite-difference (FD) wave equation modeling gives all arrivals generated by numerical solutions to the wave equation. The ray tracing helps us to identify arrivals on the FD seismograms.

Ray traced paths are governed by Snell's Law while the amplitudes can be computed by the asymptotic ray tracing amplitudes described by Červený and Ravindra (1971). For these wave paths, it is easiest to identify the modes on the wave equation calculations using ray tracing. Fig. 3 gives the PP reflections from the top of the McMurray formation along with the traveltimes for a surface source and 100 surface receivers to the right of the source with a spacing of 10 m. The traveltimes have hyperbolic NMO (normal moveout) for a velocity of 2000 m/s. Fig. 4 gives the PPPP reflections for P-waves that travel through the

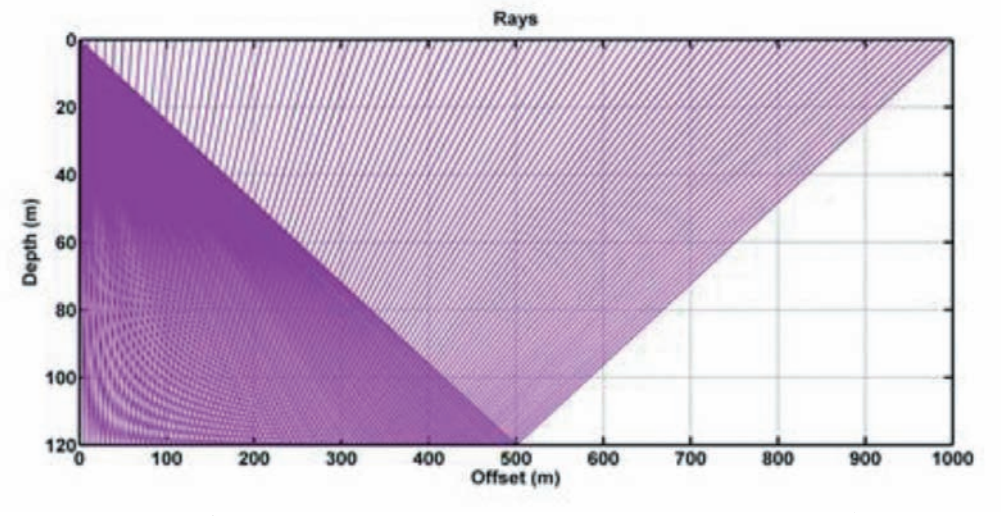

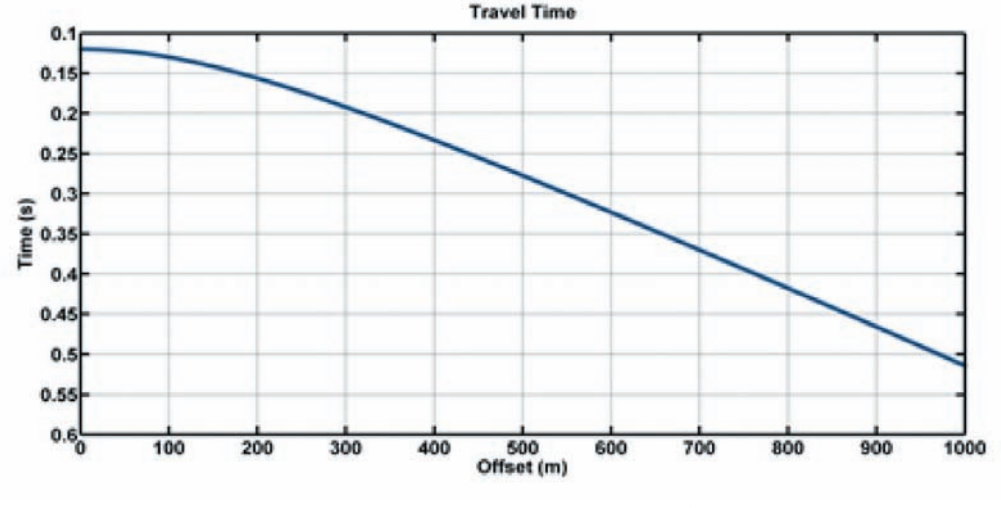

Fig. 3. (Top) The modeled ray paths for reflections from the interface between layers 1-2 in the SAGD model for a surface source at x = 0 and 100 receivers placed at 10 m intervals. (Bottom) The modeled travel times for the PP reflections from the base of the top layer in the SAGD model.

top 2 layers before being reflected from the base of McMurray - top of Devonian interface. Fig. 5 gives the ray paths and traveltimes for PSSP waves. These are waves that pass through layer 1 as P-waves before being converted to S-waves in passing through layer 2 (McMurray) and then reflected from the

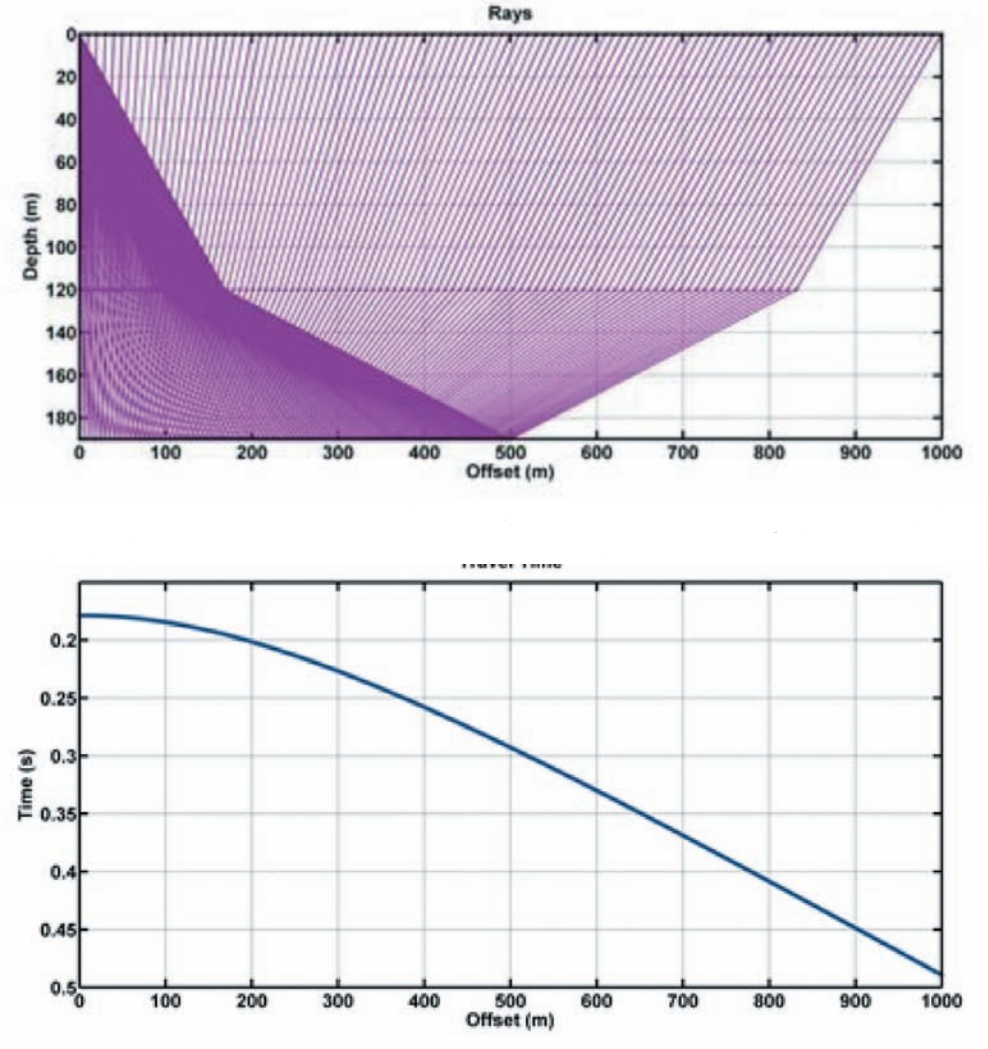

Fig. 4. (Top) Reflected rays for the PPPP reflections from interface between layers 2 and 3. (Bottom) Traveltimes for the PPPP reflections. The reflected P-waves in Figs. 3 and 4 are those generally used in seismic interpretation.

top of the Devonian formation. These PSSP arrivals have considerably more NMO than the PPPP arrivals due to spending part of their journey as a lower velocity S-wave in layer 2.

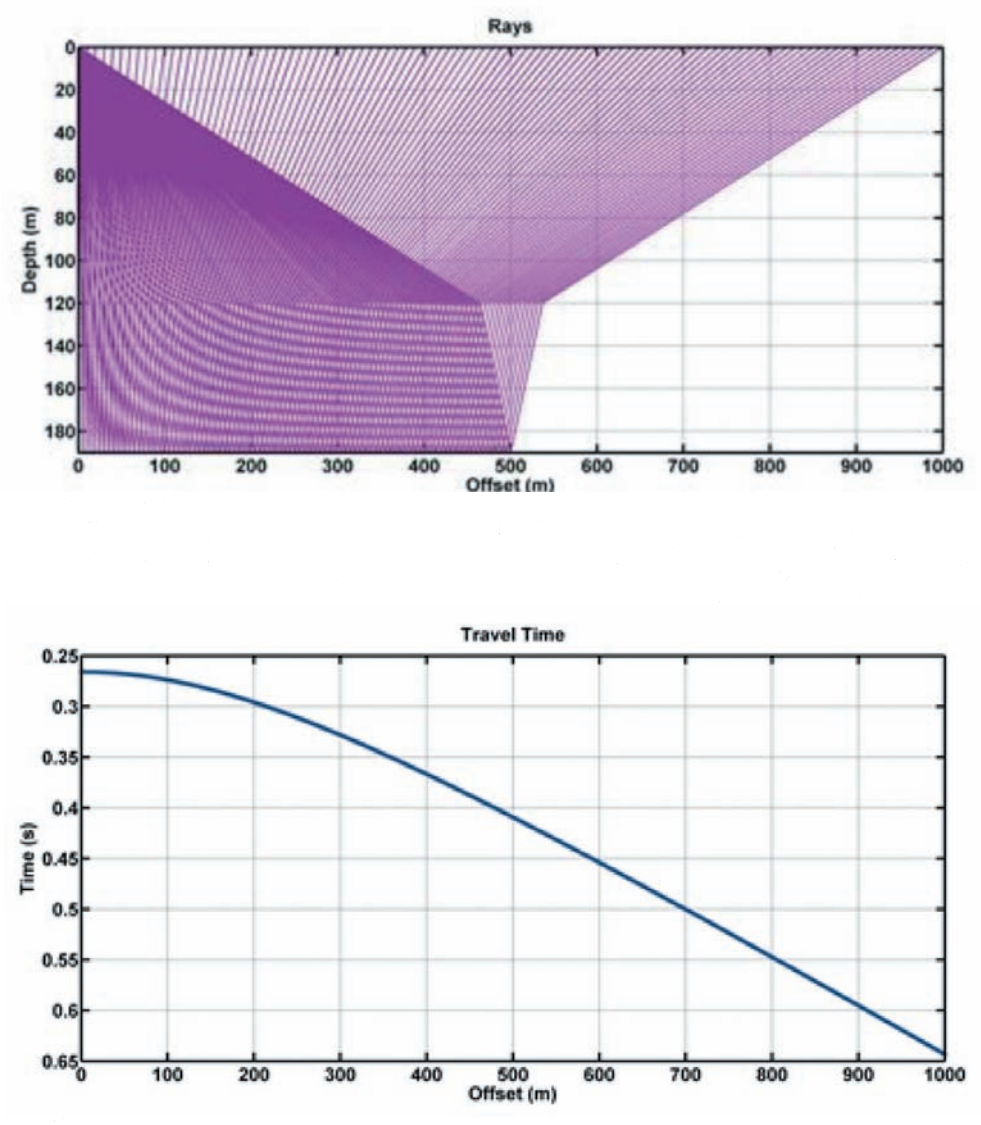

Fig. 5. (Top) Reflected rays for the PSSP mode reflected from the interface between layers 2 and 3. (Bottom) Traveltimes for the PSSP modes.

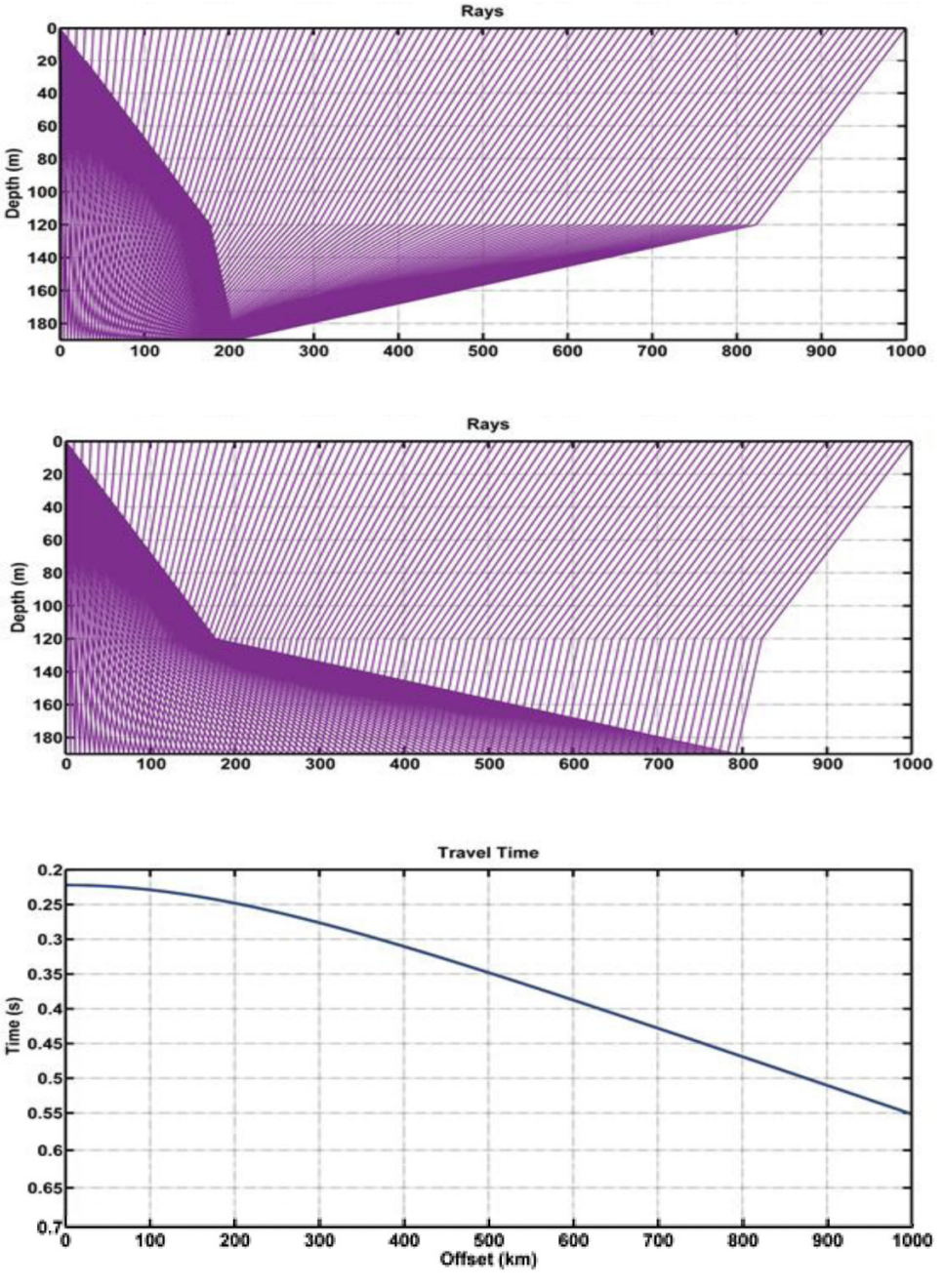

Fig. 6. The PSPP rays (top) and PPSP rays (middle) for reflections from the interface between layers 2 and 3. (Bottom) Traveltimes for the PSPP and PPSP reflections.

Other converted waves of interest include the PSPP and the PPSP rays as shown in Fig. 6. Both these waves spend only one part of their journey as S-waves in layer 2 - one wave (PSPP) has an S-component on the way down and the other (PPSP) with an S component on the way up. Both waves will have exactly the same traveltime (shown also in Fig. 6) since the total distances are the same over ray paths lengths with the same velocity. These waves will come in earlier than PSSP and will have NMO that is less than PSSP but greater than PPPP.

We have computed the ray paths for the P-wave reflections (PP, PPPP) and the various converted wave modes (PSSP, PPSP, PSPP). With ray reflectivity methods (Daley and Krebes, 2015), we can compute the amplitudes of converted modes. We do this for the recorded vertical component amplitudes. The converted wave amplitudes for PSSP and PSPP+PPSP are shown in Fig.7. As expected from the boundary conditions for 2D elastic media, there is zero

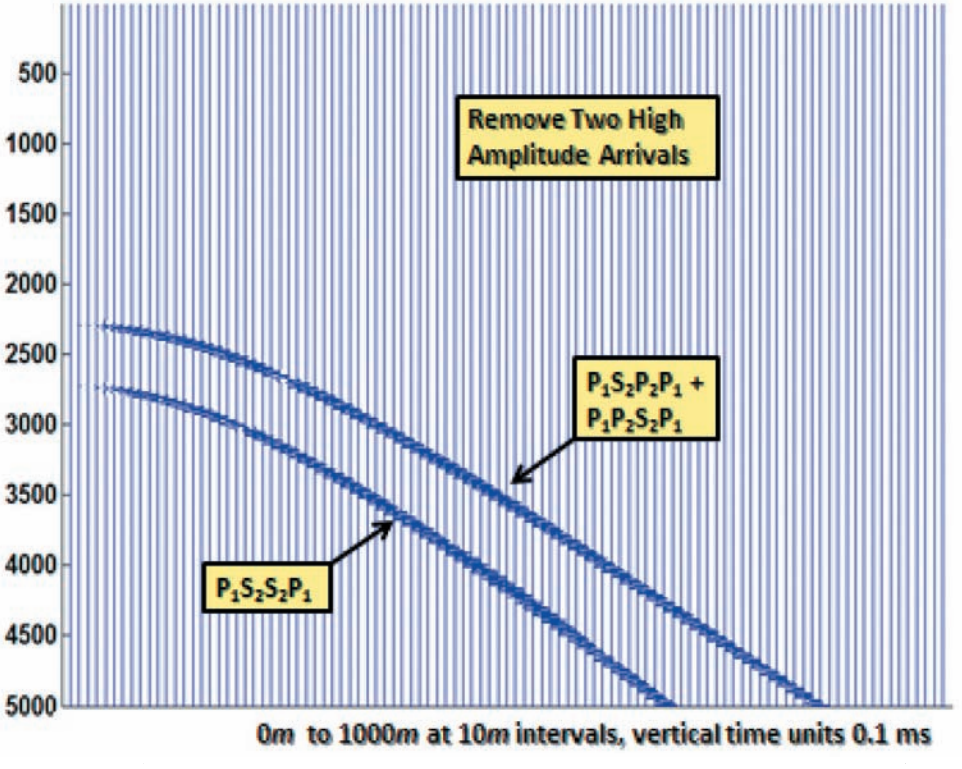

Fig. 7. Ray reflectivity amplitudes for the converted wave modes as a function of offset. Note the zero amplitudes at zero offset and the increase in amplitude with offset for both modes.

amplitude associated with converted waves for a normally incident wave on a flat boundary. Therefore, for source-receivers with zero offset, the amplitudes are zero for these normally incident waves. As seen in Fig. 7, the amplitudes for the converted modes all increase with offset. We will now examine the seismograms for waves computed using FD wave equation calculations.

Elastic wave synthetic seismograms computed by finite-differences

For modeling of P-SV waves, we use the 2D modeling code for fourth-order finite-differencing of the wave equation, as described by Levander (1988) and modified by Luo and Schuster (1991). The complete mathematical description of the staggered grid calculations for this code are described in Levander's paper.

The velocity model of the P-wave and S-wave velocities is shown in Fig.2. The vertical component of wave equation response using Levander's finite-difference algorithm is computed for a source at a depth of 10 m in the middle of a spread of 401 receivers. Receivers are all at a depth of 4 m with horizontal spacings of 1 m. The wave equation seismogram is shown in Fig. 8. As a guide to picking events on the section, the zero offset traveltimes for surface sources and receivers are the following:

1. PP reflection time is 120 ms.

2. PPPP reflection time is 178 ms.

3. PPSP and PPSP reflection times are 222 ms.

4. PSSP reflection time is 269 ms.

These traveltimes are a good guide to picking events on the FD section which are labelled in Fig. 8. (The arrivals will not be exactly the same as the above since the FD computations used a buried source and receivers and had a wavelet delay in the seismograms; nevertheless the FD seismogram is within a few ms of the above values).

In order to upscale the reflections, we can choose to filter out the direct arrivals and head waves from seismogram of Fig. 8 to emphasize the reflection events in the filtered seismogram of Fig. 9. The PSSP event (labelled in this figure) has very dim amplitudes at near offset with reflection energy being strong at far offset. According to the ray trace and the FD wave equation modeling, the PSSP reflections have considerably more NMO than the P-wave reflections. The PSSP reflection amplitudes are dim at near offset but are strong at far offset for flat reflectors.

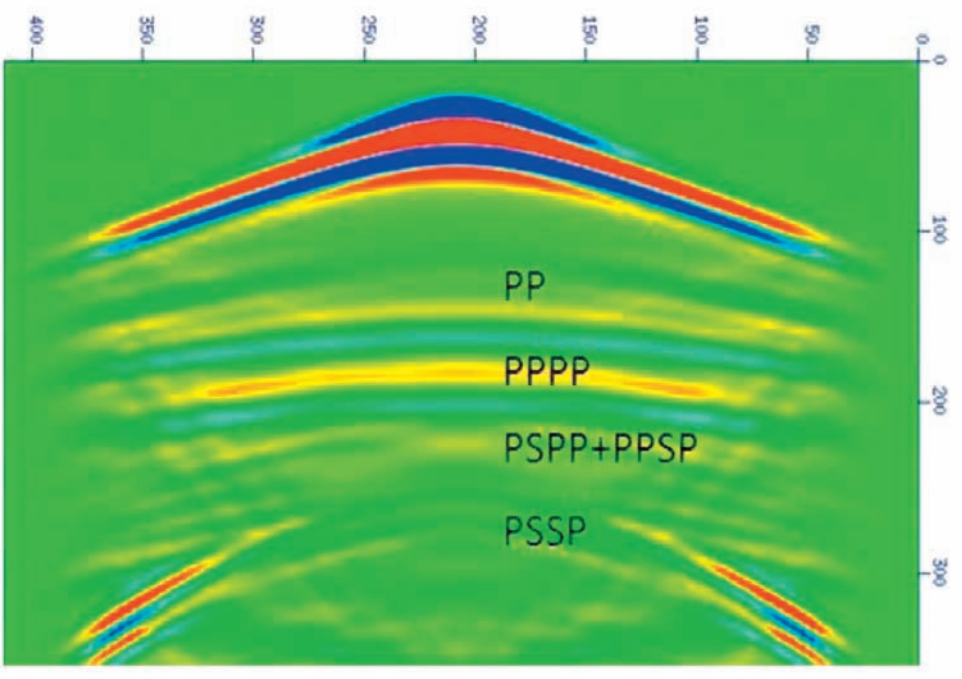

Fig. 8. FD wave equation synthetic seismogram obtaining using Levander's algorithm. Horizontal scale is in m and the vertical scale in ms. The source horizontal position is at x = 204 m and the source depth is at z = 10 m. Receivers are placed every 1 m horizontally and receivers are at a depth of 4 m.

UTILIZATION OF PSSP WAVES

Having modeled the PSSP waves, and other converted modes, with both ray tracing and FD modeling, the question arises as to whether or not these signals can be useful in determining seismic P-wave and S-wave velocities.

Suppression by NMO and stacking

The traditional approach to elastic wave inversion has been to exploit the difference in the NMO between P-wave reflections and converted wave reflections and to simply stack out the converted waves, leaving only the P-wave reflections. In other words, the converted waves are treated as undesirable signal and suppressed in the stacking process. This can be appreciated by examining

NMO corrections to the reflection seismogram of Fig. 10 (upper left). If an NMO correction is made to the seismogram with a stacking velocity of 2000m/s, the NMO correction aligns the PP reflection at 120 ms, leaving residual NMO in the PSSP event. A stack would enhance the PP reflection. If an NMO correction were made with a stacking velocity of 1500 m/s, the PP event is overcorrected but the PSSP reflection is still undercorrected. While a choice of stacking velocities could enhance the PP and PPPP reflections, this conventional processing does not utilize the PSSP energy. The stacking process would essentially treat the PSSP arrivals as undesirable signal of "noise" and attenuate the PSSP by NMO corrections for P-wave velocity and simply stacking out the PSSP arrivals. We advocate that the PSSP energy can be utilized by using full waveform inversion (FWI) following the use of conventional processing to provide a good initial model.

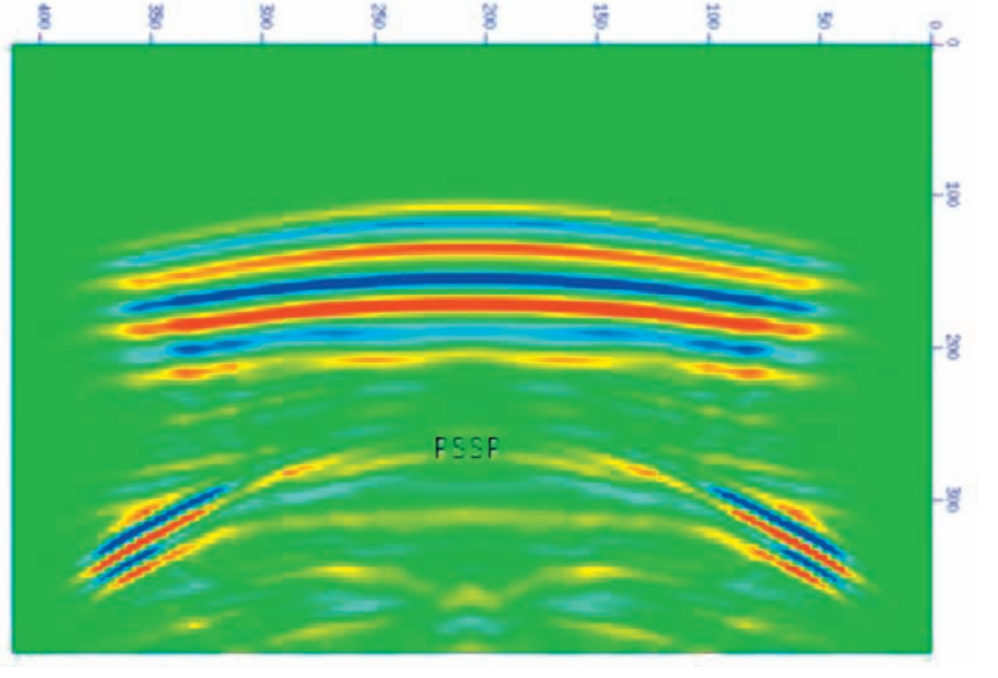

Fig. 9. FD wave equation synthetic seismogram after filtering out the direct arrivals and head waves and rescaling.

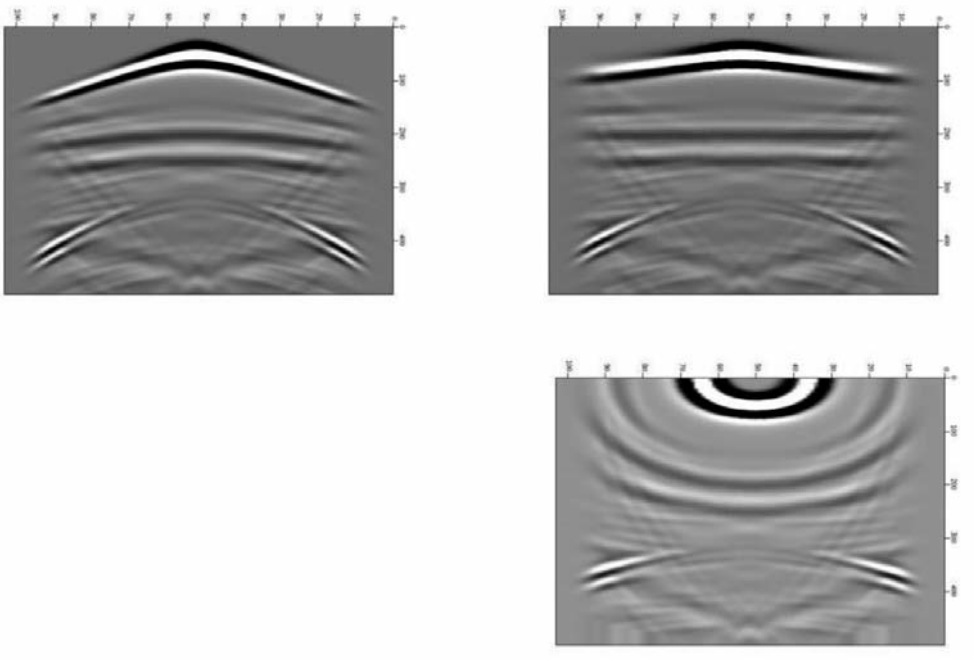

Fig. 10. NMO corrections: The vertical component seismogram prior to NMO corrections (upper left), as originally shown in Fig. 8. The upper right figure shows the seismogram after using NMO corrections for velocity of 2000 m/s. The lower right figure shows the seismogram after using NMO corrections for velocity of 1500 m/s.

Full waveform inversion (FWI)

By showing how modeling has described the converted wave energy, including PSSP arrivals, we have actually developed to tools for utilizing this converted wave energy in an inversion. Full waveform inversion attempts to match all the model response values to the data values by adjusting the model parameters, such as velocities. If **d** represents a vector containing data amplitudes and **f** represents a vector containing the model response values, we find the values of the model parameters, **x**, that will minimize the sum of squares of errors, S, between **d** and **f** values. That is, we minimize $S = [\mathbf{d}-\mathbf{f}]^2$ by computing $\partial S/\partial x_j = 0$ for all x_j. This same FWI inversion technique is applied for seismic-Q estimation by Lines et al. (2014) and the mathematical details are given in that paper. **By using conventional processing to get close to the true model, we can get closer to the true model by using the FWI technique that uses all seismic arrivals.**

A simple example of FWI inversion for using the vertical component data in our problem is illustrated in Fig. 11. For this example, we perform FWI on the synthetic data in Fig. 9. In this example we start with a an initial velocity estimate for layers that is too small by 10%. That, is the P-wave velocity of layer 1 is estimated to be 1800 m/s rather than 2000 m/s. The model response of the initial model shown in the left part of Fig. 11 and the inversion in Fig.11 is virtually identical to the desired data. By adjusting the velocity to minimize the difference between the model and data, the FWI inversion needs three iterations to adjust the velocity and the convergence to the correct model is shown in Fig. 12. After 3 iterations, FWI reaches the correct velocity and the converged model response.

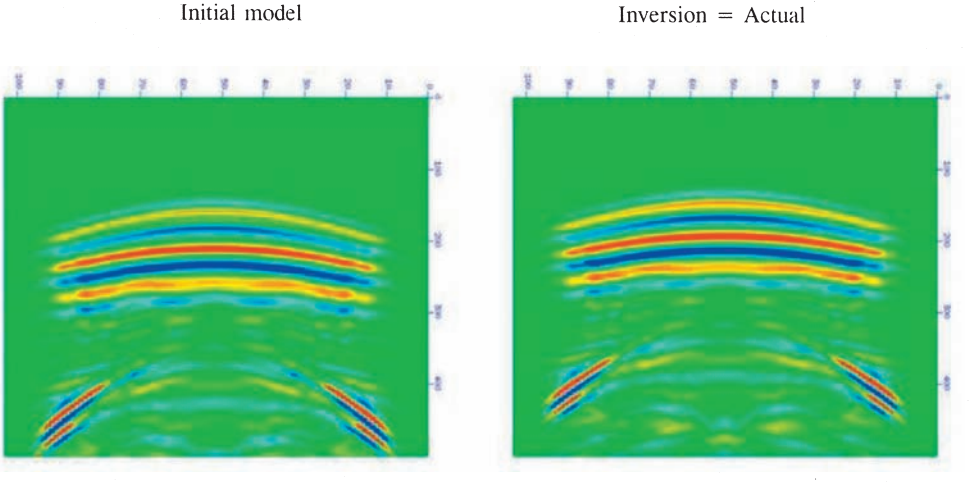

Fig. 11. (Left) Initial model response for velocity error of 10%. (Right) Full waveform inversion solution after 3 iterations.

While this is a simplistic result, it would seem that the fitting of an elastic model to the data by an iterative FWI procedure should allow us to estimate the model velocities by fitting the P-wave and converted wave arrivals. In other words, we use all arrivals in the seismogram to perform the model-based inversion.

CONCLUSIONS AND FUTURE DIRECTIONS

There are seismic events of far offset recordings with significant NMO that are due to converted waves. These arrivals can be PSSP waves as predicted by ray tracing and wave equation modeling. With traditional processing, these arrivals will be suppressed and treated as "noise" in conventional NMO stack. However, it should be worthwhile to treat these converted waves as signal and use them in full waveform inversion to improve our Earth models. For good signal-to-noise recordings, this can be achieved by the use of full-waveform inversion.

ACKNOWLEDGEMENTS

The authors would like to thank CHORUS (Consortium for Heavy Oil Research by University Scientists) and CREWES (Consortium for Research in Elastic Wave Exploration Seismology) for their financial support of this project. We also thank Dr. Ian Jones of Ion-GXT Imaging Solutions for his constructive comments and suggestions that have improved this paper.

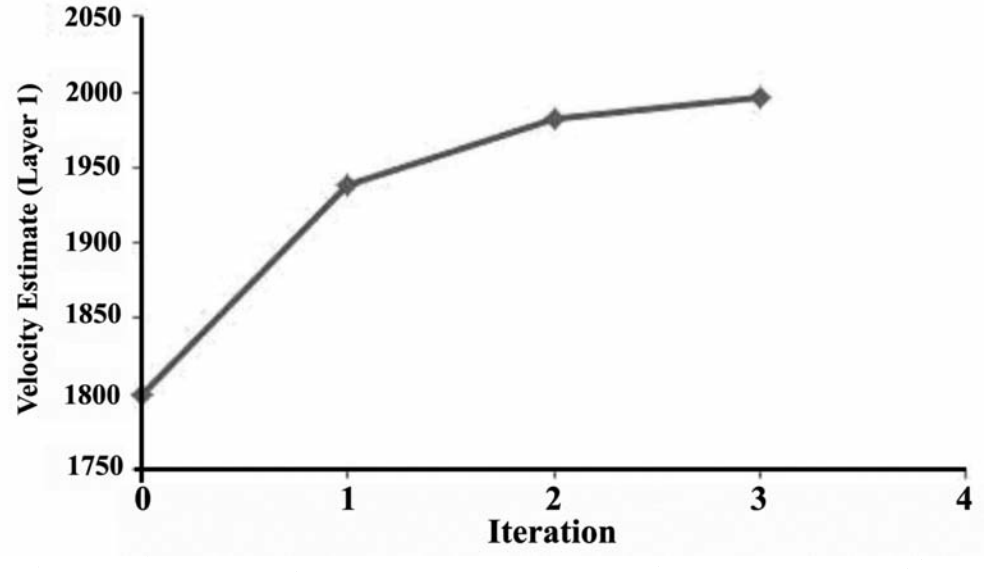

Fig. 12. Iteration to convergence - 3 iterations. Initial guess = 1800 m/s; converged estimate = 1998 m/s; actual velocity = 2000 m/s.

REFERENCES

Červený, V. and Ravindra, R., 1971. Theory of Seismic Head Waves. University of Toronto Press, Toronto.

Jones, I.F., 2014. Tutorial: the seismic response to strong vertical velocity change. First Break, 31: 79-90.

Levander, A.R., 1988. Fourth-order finite-difference P-SV seismograms. Geophysics, 53: 1425-1436.

Lines, L.R., Daley, P.F. and Ibna-Hamid, L., 2010. The accuracy of dipole sonic logs and its implications for seismic interpretation. J. Seismic Explor., 19: 87-102.

Lines, L.R., Vasheghani, F. and Bording, R.P., 2014. Short note: Seismic-Q estimation using full waveform inversion of noisy data - A feasibility study. Can. J. Explor. Geophys., 39: 15-20.

Luo, Y. and Schuster, G., 1991. Wave equation traveltime inversion. Geophysics, 56: 645-653.